

Thickness-dependence of the electronic properties in V_2O_3 thin films

C. Grygiel, Ch. Simon, B. Mercey, W. Prellier, and R. Frésard
*Laboratoire CRISMAT, UMR 6508 CNRS-ENSICAEN, 6,
Boulevard du Maréchal Juin, 14050 CAEN Cedex, France*

P. Limelette

Laboratoire LEMA, CNRS-CEA UMR 6157, Université F. Rabelais, Parc de Grandmont, 37200 TOURS, France

(Dated: October 31, 2018)

High quality vanadium sesquioxide V_2O_3 films (170-1100 Å) were grown using the pulsed laser deposition technique on (0001)-oriented sapphire substrates, and the effects of film thickness on the lattice strain and electronic properties were examined. X-ray diffraction indicates that there is an in-plane compressive lattice parameter (a), "close to -3.5% with respect to the substrate" and an out-of-plane tensile lattice parameter (c). The thin film samples display metallic character between 2-300 K, and no metal-to-insulator transition is observed. At low temperature, the V_2O_3 films behave as a strongly correlated metal, and the resistivity (ρ) follows the equation $\rho = \rho_0 + A \cdot T^2$, where A is the transport coefficient in a Fermi liquid. Typical values of A have been calculated to be $0.14 \mu\Omega \text{ cm K}^{-2}$, which is in agreement with the coefficient reported for V_2O_3 single crystals under high pressure. Moreover, a strong temperature-dependence of the Hall resistance confirms the electronic correlations of these V_2O_3 thin films samples.

PACS numbers: 81.15.Fg, 71.27.+a, 74.20.Mn, 68.55.-a

First discovered by Foex in 1946,¹ vanadium sesquioxide V_2O_3 has received a great deal of attention, both by theoreticians as well as experimentalists. Indeed, it has been recognized previously that a pressure-induced metal-to-insulator transition (MIT) for V_2O_3 is driven by electron correlation,² establishing V_2O_3 as a prototypical strongly correlated electron system. As a result, numerous studies on the effect of composition or external parameters on the transport properties of V_2O_3 have been reported.^{3,4,5} Particular attention has been also paid to the phase transitions of V_2O_3 : in the pressure-temperature plane two phase transitions are reported, either when applying a hydrostatic pressure or a chemical pressure (see for example, $(V_{1-x}M_x)_2O_3$ with $M = \text{Cr, Ti, ...}$).^{3,4} For example, a system that is close to all phase boundaries is $(V_{0.985}\text{Cr}_{0.015})_2O_3$ at 200 K.⁶ When the temperature is decreased, this paramagnetic metal undergoes a first order phase transition from a corundum structure with rhombohedral symmetry ($R\bar{3}c$ space group, with $a = 4.951 \text{ \AA}$, $c = 14.003 \text{ \AA}$) to an antiferromagnetic insulator with monoclinic structure ($I2/a$).⁷ When the temperature or the Cr-content is increased, a paramagnetic metal to paramagnetic insulator transition takes place.⁶ While the former transition bears strong similarities with many usual magnetic transitions, the latter one corresponds to the famous Mott transition. Qualitatively, this Mott transition is well described by the Hubbard model: increasing the Cr-content results in increasing the ratio U/W (U being the strength of the Coulomb interaction, and W the bandwidth), in which case the quasiparticle residue decreases, and eventually vanishes at the MIT.⁸ Furthermore, when considering the optical conductivity, the optical weight at low energy is transferred to energies of order U .⁹ When the system is close to the Mott point, thermal fluctuations destabilize the

coherence of the Fermi liquid (FL), and an increase in temperature results into a MIT.^{10,11,12} Several orbitals are involved at the Fermi energy, and however, a quantitative description of V_2O_3 needs to build on a more involved theory, such as the one pioneered by Held *et al.*¹³

Despite extensive studies on polycrystalline powder and single crystal V_2O_3 samples,^{14,15,16,17} there have been few reports on thin film samples. Schuler *et al.* addressed the influence of the synthesis conditions upon the classical metal-to-insulator transition and the growth modes of the films.¹⁸ The relation between the transition temperatures and the lattice parameters also have been reported.^{19,20,21} There is little knowledge however on the thickness-dependence of the properties of the V_2O_3 thin films.

In this letter, we examine a series of epitaxial V_2O_3 thin films, including their lattice parameters, roughness, and Hall resistance, in order to investigate their transport properties as a function of thickness.

Samples of V_2O_3 thin films, of which the thickness ranged from 170 Å to 1100 Å, were grown on (0001)-oriented Al_2O_3 substrates (rhombohedral with the parameters, $a = 4.758 \text{ \AA}$, $c = 12.991 \text{ \AA}$) by the pulsed laser deposition technique. A pulsed KrF excimer laser (Lambda Physik, Compex, $\lambda = 248 \text{ nm}$) was focused onto a stoichiometric V_2O_5 target at a fluence of 4 J cm^{-2} with a repetition rate of 3 Hz. The substrate heater was kept at a constant temperature ranging from 600°C to 650°C . A background of argon pressure around 0.02 mbar was applied inside the chamber. At the end of the deposition, the film was cooled down to room temperature at a rate of 10 K min^{-1} under a 0.02 mbar argon pressure. The film thickness was determined, to an uncertainty below two V_2O_3 unit cells, by a mechanical stylus measuring system

(Dektak³ST). The structure of the films was examined by X-Ray Diffraction (XRD, with the Cu $K\alpha_1$ radiation, $\lambda=1.54056$ Å) using a Seifert 3000P diffractometer for the out-of-plane measurements and a Philips X'Pert for the in-plane measurements. In-plane a lattice parameters were extracted from (104) , (116) , (113) asymmetric reflections. The resistivity of the samples were measured in four probe configuration using a PPMS system. To make appropriate connections onto the film, four silver plots were first deposited via thermal evaporation onto the film, and then thin aluminum contact wires were used to connect these areas to the electrodes. For Hall effect measurements, a Van der Pauw configuration of silver plots was used. For each temperature value, the transverse resistance is measured with an applied magnetic field varying from -7 T up to $+7$ T. The Hall resistance R_H is calculated from the transverse resistance (R_{xy}) using the formula $R_H=(t \cdot R_{xy})/H$, where H is the applied magnetic field.

As it is known that the nonstoichiometry can drastically influence the electric properties of V_2O_3 ,¹⁵ a X-ray photoelectron spectroscopy study was carried out. It shows that the oxidation state of vanadium can be estimated around $+3$, confirming that the films stoichiometry is close to V_2O_3 .¹⁹ $\Theta - 2\Theta$ scans XRD measurements reveal that only the peaks corresponding to the $00l$ reflections (where $l=6, 12, \dots$) are present, which indicates that the c -axis of the films is perpendicular to the plane of the substrate. Φ -scans, recorded around the (104) reflection show three peaks separated by 120° from each other, indicating that the films have a 3-fold symmetry and are grown epitaxially, with respect to the substrate. These results are in agreement with the rhombohedral symmetry observed in the bulk V_2O_3 . This symmetry and the $R\bar{3}c$ space group are further confirmed by electron diffraction pattern analyses. The high quality of the films was also attested by the low value of the rocking-curve close to (0.20°) measured around the (006) reflection of the film.

Fig. 1 displays the evolution of the lattice parameters (c) and (a), characteristic of the $R\bar{3}c$ structure, as a function of the thickness t . The out-of-plane lattice parameter (c) is slightly larger than the bulk values, by 0.45 ± 0.1 %, while the in-plane (a) is smaller by -0.55 ± 0.1 %, confirming a biaxial compression in the (ab) plane, estimated to -3.5 ± 0.5 % with respect to the substrate (the stress values are calculated from the mean-values (c) and (a) obtained from the thickness dependence in Fig. 1). This suggests an anisotropic strain similarly to previous reports.²⁰ Surprisingly, the lattice parameters are almost independent of t , indicating that the films are fully strained in the whole thickness range. The surface morphology was also studied by Atomic Force Microscopy (AFM) with a scan area of $3 \times 3 \mu\text{m}^2$. Topography of the V_2O_3 samples reveals that the roughness increases when the thickness increases. For example, a typical surface roughness (rms) of 4.5 Å was observed for the thinnest film (170 Å), while a thicker sample (700 Å) has a rms

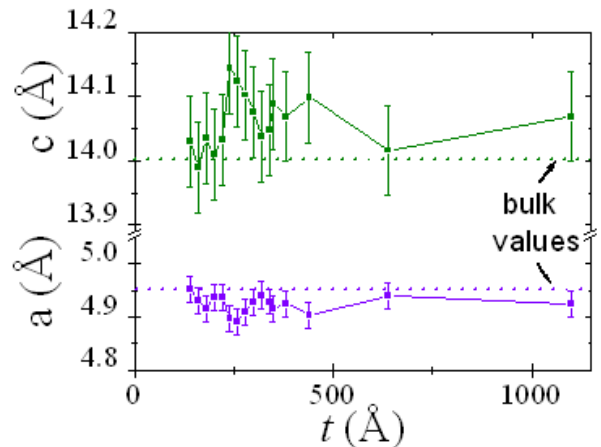


Figure 1: Thickness-dependence of the a , c lattice parameters. Dotted lines indicate the bulk values. The line is a guide for the eye only.

value of 11 Å. This may indicate that the growth mode is mixed: a layer-by-layer (2D-mode) on the (ab) plane at the initial step of the growth, and an island coalescence (3D-mode) along the c -axis when the thickness increases. To summarize, the structural and microstructural analyses confirm that the films crystallize in the $R\bar{3}c$ structure, as in bulk, despite a large in-plane compressive strain.

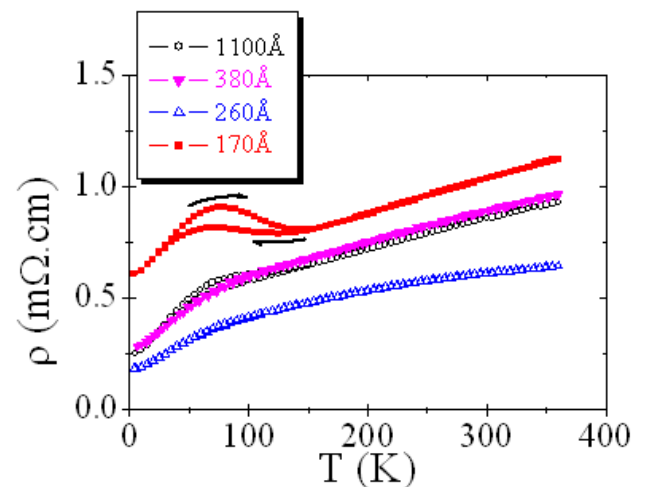


Figure 2: Temperature-dependence of the longitudinal resistivity of several V_2O_3 thin films.

The longitudinal resistivity (ρ) of V_2O_3 films is plotted in Fig. 2 as a function of temperature for several thicknesses. In contrast to bulk samples, none of the investigated films exhibit a strong temperature-dependent

resistivity. This is especially valid for $t > 220 \text{ \AA}$, in which case the resistivity increases continuously with temperature as in a metal. Nevertheless, some hysteresis is observed, though strongly suppressed with respect to the bulk. Thus, we can conjecture that the abovefound stress in the (ab) plane results into a larger band width, and hinders the paramagnetic metal-to-antiferromagnetic insulator transition. In contrast, for thinner films ($t < 220 \text{ \AA}$), the films are metallic with a weak increase of the resistivity near 150K . Its origin might be a reminder of the structural transition. As shown in Fig. 3, resistiv-

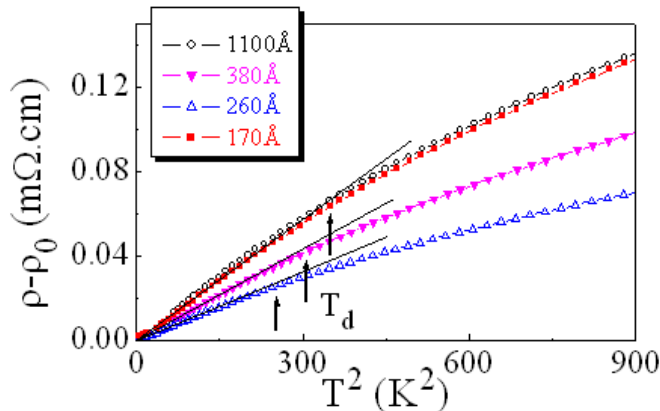


Figure 3: Resistivity versus T^2 in the low temperature region. The T_d temperature (see text for details) is also indicated.

ity data for all films follow a law in $\rho = \rho_0 + A \cdot T^2$ in the temperature range from 2K up to a characteristic temperature T_d . Here ρ_0 represents the (film dependent) residual resistivity, and A the transport coefficient in a Fermi liquid. This behavior, which differs from simple metals that exhibit T^3 or T^5 behavior, is seldom observed over such a temperature range, except for a few strongly correlated electron system, such as $\text{Ca}_3\text{Co}_4\text{O}_9$.²² Table I summarizes the values (ρ_0), (A) and (T_d) for a series of films. The average value of A is close to $0.14 \mu\Omega \text{ cm K}^{-2}$ across the whole thickness range, indicating that the A coefficient is not *significantly* thickness-dependent. Moreover, it should be noted that such values are similar to those measured for single crystal V_2O_3 samples

Table I: Thickness t , residual resistivity ρ_0 , Fermi liquid transport coefficient A/A_0 (with $A_0 = 10^{-5} \text{ m}\Omega \text{ cm K}^{-2}$), temperature T_d , carriers number at 300 K n , and Hall mobility at 300 K μ_H for three films.

t (\AA)	ρ_0 ($\text{m}\Omega \text{ cm}$)	A/A_0	T_d (K)	n (cm^{-3})	μ_H ($\text{cm}^2 (\text{Vs})^{-1}$)
1100	0.24	19.6	18.7	4.5 ± 0.210^{22}	0.16 ± 0.05
380	0.27	14.0	17.5	4.4 ± 0.410^{22}	0.15 ± 0.06
260	0.19	10.2	15.8	4.9 ± 0.510^{22}	0.21 ± 0.10

subjected to high pressures (26-52 kbar).¹⁷ The high A values involve the existence of strong electronic correlations in our metallic thin films. The product $A \cdot (T_d)^2 / a$ is about two orders of magnitude lower than h/e^2 , indicating that the FL behavior does not extend up to the effective Fermi temperature. Instead, an additional scattering channel opens up at $T > T_d$, which might be provided by spin fluctuations. To better quantify the temperature range where this scattering channel is relevant, we performed Hall effect measurements in the temperature range 2-300 K. Fig. 4 shows the resulting Hall resistance (R_H) for a series of films.

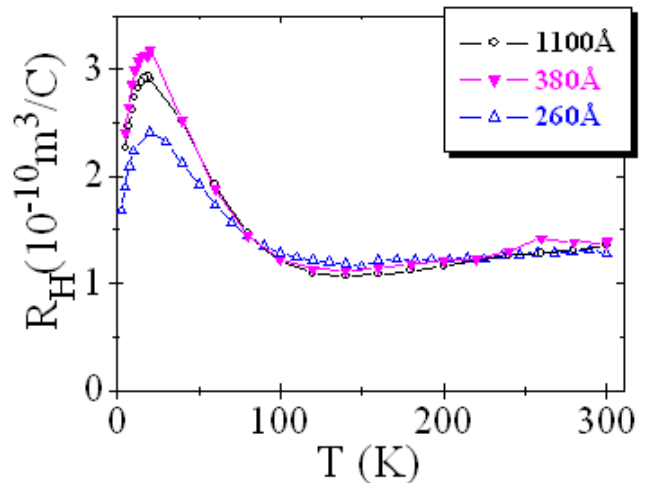


Figure 4: Temperature-dependence of the Hall resistance of several V_2O_3 thin films.

The positive slope of the Hall resistance implies hole-like charge carriers, as inferred by McWhan *et al.*¹⁴ Moreover, while the Hall resistance would be nearly temperature independent in a regular metal, it here exhibits a strong temperature dependence, especially for $T < 200 \text{ K}$. In particular, the strain involved in our films has little influence on the location of the maximum of R_H , as it is located at a temperature very close to the one reported for metallic bulk samples.²³ Nevertheless, this temperature slightly increases as the thickness decreases. A similar result has been observed in the aforementioned single crystals with an increase in pressure, indicating that the decrease of the thickness is consistent with an increase of the pressure. At room temperature, in the temperature-independent regime, the values of the carriers number (n) and Hall mobility (μ_H) can also be extracted from the Hall resistance value (see Table I). For the thicker film (1100 \AA), they are calculated to be $n = 4.5 \pm 0.210^{22} \text{ cm}^{-3}$ and $\mu_H = 0.16 \pm 0.05 \text{ cm}^2 \text{ V}^{-1} \text{ s}^{-1}$, which are consistent with the ones observed in V_2O_3 single crystals.¹⁴ Note that R_H loses its temperature-dependence above $\sim 200 \text{ K}$, which indicates that above this temperature the correlation length of the fluctua-

tions that scatter the electrons become of the order of the lattice parameter. Consequently, in this regime, the resistivity is expected to be T -linear, which is indeed observed for most of the films.

In summary, high quality epitaxial V_2O_3 thin films were grown, with thickness ranging from 170-1100 Å, by pulsed laser deposition on sapphire substrate (0001- Al_2O_3). Using multiple of characterization techniques, we confirm that the films have the same rhombohedral structure ($R\bar{3}c$ space group) as in the bulk despite the substrate-induced strains. The thickness-dependence of the electronic properties show the suppression of the clas-

sical metal-to-insulator transition with a metal-like behavior. At low temperature, the dependence of the resistivity as a function of T^2 was measured to be that of a strong correlated metal, and was confirmed by temperature-dependence of the Hall resistance.

We thank D. Grebille and A. Pautrat for fruitful discussions. J.F. Hamet and Y. Thimont are also acknowledged for the AFM measurements. This work is carried out in the frame of the STREP CoMePhS (NMP3-CT-2005-517039) supported by the European community and by the CNRS, France.

-
- ¹ M. Foex, C. R. Acad. Sci. **223**, 1126 (1946).
² N. F. Mott, Proc. Phys. Soc. A **62**, 416 (1949).
³ D. B. McWhan, A. Menth, J. P. Remeika, W. F. Brinkman, and T. M. Rice, Phys. Rev. B **7**, 1920 (1973).
⁴ M. Yethiraj, J. Solid State Chem. **88**, 53 (1990).
⁵ P. Limelette, A. Georges, D. Jérôme, P. Wzietek, P. Metcalf, and J. M. Honig, Science **302**, 89 (2003).
⁶ H. Kuwamoto, J. M. Honig, and J. Appel, Phys. Rev. B **22**, 2626 (1980).
⁷ P. Dernier and M. Marezio, Phys. Rev. B **2**, 3771 (1970).
⁸ W. F. Brinkman and T. M. Rice, Phys. Rev. B **2**, 4302 (1970).
⁹ G. A. Thomas, D. H. Rapkine, S. A. Carter, A. J. Millis, T. F. Rosenbaum, P. Metcalf, and J. M. Honig, Phys. Rev. Lett. **73**, 1529 (1994).
¹⁰ J. Spalek, A. Datta, and J. M. Honig, Phys. Rev. Lett. **59**, 728 (1987).
¹¹ A. Georges, G. Kotliar, W. Krauth, and M. J. Rozenberg, Rev. Mod. Phys. **68**, 13 (1996).
¹² R. Frésard and G. Kotliar, Phys. Rev. B **56**, 12 909 (1997).
¹³ K. Held, G. Keller, V. Eyert, D. Vollhardt, and V. I. Anisimov, Phys. Rev. Lett. **86**, 5345 (2001).
¹⁴ D. B. McWhan and J. P. Remeika, Phys. Rev. B **2**, 3734 (1970).
¹⁵ Y. Ueda, K. Kosuge, and S. Kachi, J. Solid State Chem. **31**, 171(1980).
¹⁶ S. A. Shivashankar and J. M. Honig, Phys. Rev. B **28**, 5695 (1983).
¹⁷ D. B. McWhan and T. M. Rice, Phys. Rev. Lett. **22**, 887 (1969).
¹⁸ H. Schuler, S. Klimm, G. Weissmann, C. Renner, and S. Horn, Thin Solid Films **299**, 119 (1997).
¹⁹ S. Autier-Laurent, B. Mercey, D. Chippaux, P. Limelette, and Ch. Simon, Phys. Rev. B **74**, 195109 (2006).
²⁰ S. Yonezawa, Y. Muraoka, Y. Ueda, and Z. Hiroi, Sol. State Comm. **129**, 245 (2004).
²¹ Q. Luo, Q. Guo, and E. G. Wang, Appl. Phys. Lett. **84**, 2337 (2004).
²² P. Limelette, V. Hardy, P. Auban-Senzier, D. Jérôme, D. Flahaut, S. Hébert, R. Frésard, Ch. Simon, J. Noudem and A. Maignan, Phys. Rev. B **71**, 233108 (2005).
²³ S. A. Carter, T. F. Rosenbaum, P. Metcalf, J. M. Honig and J. Spalek, Phys. Rev. B **48**, 16841 (1993).